Research Journal of Earth Sciences 3 (2): 63-70, 2011
ISSN 1995-9044

A New Approach for the Investigation of the Multifractality of Borehole Wire-Line Logs

S. Gaci and N. Zaourar

Département Géophysique- FSTAT- Université Des Sciences De La Terre
De Houari Boumédienne (USTHB)-Algiers, Algeria

Abstract: In previous researches, borehole wire-line logs were described as fractional Brownian motions characterized by Hurst (or Hölder) exponents which measure their global regularity degrees. Since theses monofractals are everywhere singular with the same Hurst exponent, they do not reflect the depth-evolution of the local regularity of the logs. For this purpose, we suggest a general framework, multifractional Brownian motion, to describe well logs and propose an algorithm based on the Generalized Quadratic Variations to estimate the local Hurst exponent function. Firstly, synthetic log data simulated by the Successive Random Additions method are used to assess the potential of this algorithm; it is observed that the estimated Hurst functions (or regularity profiles) are very close to the theoretical Hurst functions. Secondly, this analysis is extended to sonic logs data recorded in the KTB pilot borehole. The obtained regularity profiles allow to perform a lithological segmentation and to identify fault contacts on the geological layers crossed by the well. A strong correlation between the Hurst value variation and the lithological change is also noted.

Keys words: Well-Logs % Hurst exponent % Fractal % Multifractional

INTRODUCTION

Borehole measurements are an essential complement to exploration activities (seismic, drilling…etc) because they provide additional information from the borehole that cannot be derived from other sub-surface investigations. The analysis of these recorded data may bring supplementary information about the earth's heterogeneities.

Numerous studies have shown that borehole wire-line logs may be described by non-stationary fractional Brownian motions (fBms). These monofractal processes are characterized by a fractal k^{-2H-1}-power spectrum model where k is the wavenumber and H is the Hurst (or Hölder) exponent [1-5].

The Hurst parameter H gives an indication about the self-similarity degree and long-range dependence of the well log. When $H = 1/2$, the process is reduced to the ordinary Brownian motion (namely the process has no memory); for $H > 1/2$, it is characterized by a persistence (positive or negative)- namely the process shows a clear trend; and finally, for $H < 1/2$, it exhibits an anti-persistent behaviour. From a geometrical point of view, H determines the (constant) regularity degree of the sample paths of the fBm and is linked to the fractal Dimension D of the graph by this relation: $D = 2 - H$. The estimation of the H parameter can be carried out using several methods [6-11, 2, 3].

Indeed, the H coefficient measures the global regularity degree of the process and does not suit to study well- logs whose the local regularity varies rapidly in depth. This calls for the use of a multifractal description which consists in defining a procedure to estimate the global repartition of the various Hurst (or Hölder) exponents, but not their location.

Recently, developed stochastic models and associated regularity estimation methods allow to investigate the depth-evolution of the local regularity even on extremely erratic data. Specifically, in the present paper, we will consider the multifractional Brownian motion (mBm) as a model for borehole logs and use an estimation algorithm based on the Generalized Quadratic Variations (GQV).

The present paper is organized as fellows. First of all, we present shortly the description of the multifractional Brownian motion (mBm) model and the Generalized Quadratic Variations algorithm. Then, we show the results obtained by this technique on synthetic data simulated by Successive Random Additions (SRA) algorithm. Finally, the GQV algorithm is implemented on P and S-wave sonic measurements recorded in the KTB pilot borehole.

Corresponding Author: S. Gaci, Département Géophysique- FSTAT- Université Des Sciences De La Terre De Houari Boumédienne (USTHB)-Algiers, Algeria.

THEORY

Multifractional Brownian Motion: One of the models which can be used to describe the behaviour of the borehole wire-line logs is the multifractional Browniam motion (mBm), which generalizes the fractional Brownian motion (fBm). Then the introduction of the mBm requires the recalling of the main features of its famous special case (fBm).

Defined by Mandelbrot and Van Ness [12], the fBm is characterized by a slowly decaying autocorrelation function depending on the parameter $0 < H < 1$, named Hurst (or Hölder) exponent and admits the following moving average representation:

$$B_H(t) = G\int_{-\infty}^{0}\left[(t-s)^{H-1/2} - (-s)^{H-1/2}\right]\,dB(s) + \int_{0}^{t}\left[(t-s)^{H-1/2}\right]\,dB(s) \text{ and } B_H(0) = 0 \tag{1}$$

Where dB stands for the ordinary Brownian motion process motion and G represents a strictly-positive scaling parameter: $G = C\,('(2H+1)\sin(\pi H))^{1/2}\,\&\,'(H+1/2)$ with C is a positive constant. If G = 1, the motion is said standard.

The process $B_H(t)$ is self-similar of parameter H and has stationary increments. Its covariance function is expressed:

$$Cov\left(B_H(t),\, B_H(s)\right) = \mathrm{E}\left(B_H(t)\,B_H(s)\right) = \frac{C^2}{2}\left(|t|^{2H} + |s|^{2H} - |t-s|^{2H}\right) \tag{2}$$

The fBm can be generalized by replacing the constant Hurst parameter H by a function H(t). This extension leads to define the mBm which has the following representation [13-15].

$$W_{H(t)}(t) = G\left(H(t)\right)\int_{-\infty}^{0}\left[(t-s)^{H(t)-1/2} - (-s)^{H(t)-1/2}\right]\,dB(s) + \int_{0}^{t}\left[(t-s)^{H(t)-1/2}\right]\,dB(s) \tag{3}$$

Where H: [0,4[6]0,1] is required to be a Hölder function of order $0 < 0 \# 1$ to ensure the continuity of the motion. In the case of the Hurst function $H(t)$ is constant, $W_{H(t)}(t)$ is reduced to a simple fBm.

The mBm's increments are in general neither independent nor stationary. It can be shown that they display long range dependence for all admissible non-constant regularity functions $H(t)$ [16].

Contrarily to fBm, the pointwise Hölder exponent of $W_{H(t)}(t)$, $\alpha_W = \{\alpha_W(t), t \in R\}$, may depend on the location. It equals with probability one to $H(t)$ for each t [17, 18, 19, 15].

$$\alpha_W(t) = H(t) \tag{4}$$

Thus, mBm allows to describe and to model phenomena whose regularity varies in time/space. Recall that the pointwise Hölder exponent of a stochastic process X at t_0 is defined by:

$$\alpha_X(t_0, w) = \sup\left\{\alpha > 0,\ \limsup_{h\to 0}\frac{|X(t_0+h, w) - X(t_0, w)|}{|h|^{\alpha}} = 0\right\} \tag{5}$$

Another important property of mBm is that it does not remain self-similar but is Locally Asymptotically Self-Similar (in short LASS). That means that for each t, there is an fBm of Hurst parameter H(t), which is tangent to mBm [19-21].

Local Regularity Estimation: Ayache and Lévy-Véhel [22] suggested a parametrical method to identify the Hölder exponent of mBm processes. This method is based on the computation of the so-called "Generalized Quadratic Variations" (GQV).

For a trajectory of the process $\{X(t)\}_{t\in[0,1]}$, discretized at times $\frac{p}{N}$, p , 0,..., $N-1$ with $N \$ 1$, the GQV are defined by:

$$\tilde{V}_N(t) = \sum_{p\in\tilde{u}_N(t)}\left(X\left(\frac{p}{N^d}\right) - 2X\left(\frac{p+1}{N^d}\right) + X\left(\frac{p+2}{N^d}\right)\right)^2 \tag{6}$$

Where $\tilde{u}_N(t) = \left\{p \in \mathrm{N}; 0 \le p \le N-2 \text{ and } \left|t - \frac{p}{N^d}\right| \le N^{-g}\right\}$ can be considered as ''the neighborhood'' of t.

The authors demonstrated that under some conditions imposed on the constants, (and *, the following relation is satisfied with probability one for any mBm $W_{H(t)}(t)$.

$$\lim_{n\to\infty} \frac{1}{2d}\left((1-g)-\frac{\log \tilde{V}_N(t)}{\log N}\right)=H(t) \quad (7)$$

Consequently, an estimation algorithm of the local Hölder exponent of an mBm $W_{H(t)}(t)$, called here GQV algorithm, is resulted:

$$H(t)=\frac{1}{2d}\left((1-g)-\frac{\log \tilde{V}_N(t)}{\log N}\right) \quad (8)$$

APPLICATION TO SIMULATED LOG DATA

In this section, the GQV algorithm is tested on synthetic log data which are generated by the means of the Successive Random Additions (SRA) method [23].

In order to assess the convergence of the estimator, we generated 1000 realizations of an mBm path corresponding to a four-layers geological model whose the parameters are given by the Table 1. Then, using the Hurst values estimated at four fixed positions so that each layer is represented by a position, we plotted histograms representing the Hurst values obtained by the GQV algorithm versus the realizations number for each position (Fig. 1).

Table 1: Synthetic a four-layers geological model parameters

Layers	L1	L2	L3	L4
Samples number	512	512	512	512
Ranges of Layers' indexes	1-512	513-1024	1025-1536	1537-2048
Theoretical H-value	0.2	0.4	0.6	0.8

We remark that for each position, the estimated Hurst values follow a gaussian distribution centred at a Hurst value very close to the theoretical Hurst value of the considered layer. Moreover, the bias value varies slightly with the considered position but remains small.

In addition, we simulated paths of mBms using four types of Hurst functions: linear H_1, periodic H_2, logistic H_3 and synthetic H_4 (Fig. 2) defined:

- $H_1(t) = 0.2 + 0.6t$;
- $H_2(t) = 0.5 + 0.3 \sin(4B\, t)$;
- $H_3(t)=0.3+\frac{0.3}{1+e^{-100(t-7)}}$;
- $H_4(t)=0.25+0.25t^2\left(1-\cos\left(\frac{5p}{1+e^{-20(t-0.6)}}\right)\right)$.

Then, we estimated the Hurst functions of the generated mBms owing to the GQV algorithm. Finally, for each mBm, we calculated the error function which represents the difference between the estimated Hurst function and the theoretical Hurst function.

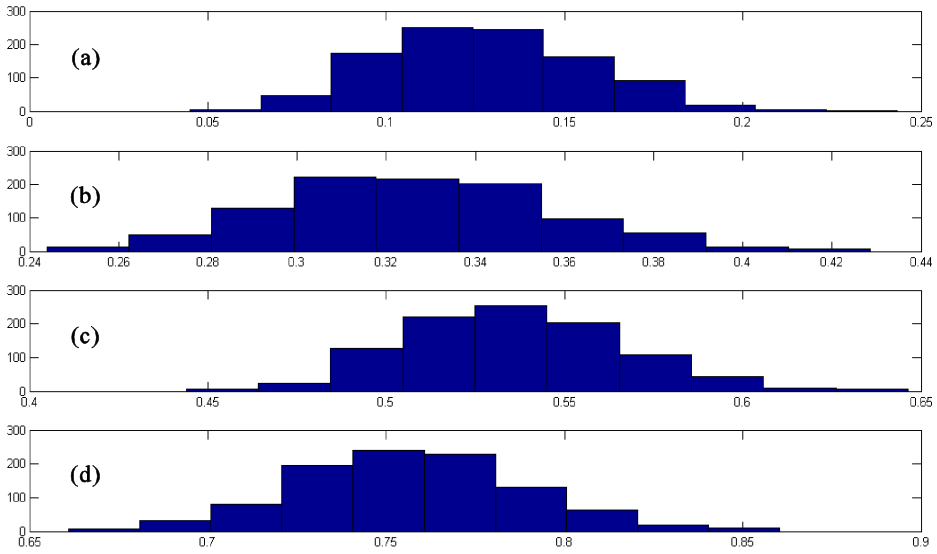

Fig. 1: Histograms of the Hurst values obtained by the GQV algorithm versus the realizations number. The four histograms are resulted from 1000 realizations of a simulated mBm s(z) corresponding to a 4-layers geological model at four positions located in (a) 1st layer; (b) 2nd layer; (c) 3rd layer and (d) 4th layer whose the theoretical H-values are respectively 0.2, 0.4, 0.6 and 0.8.

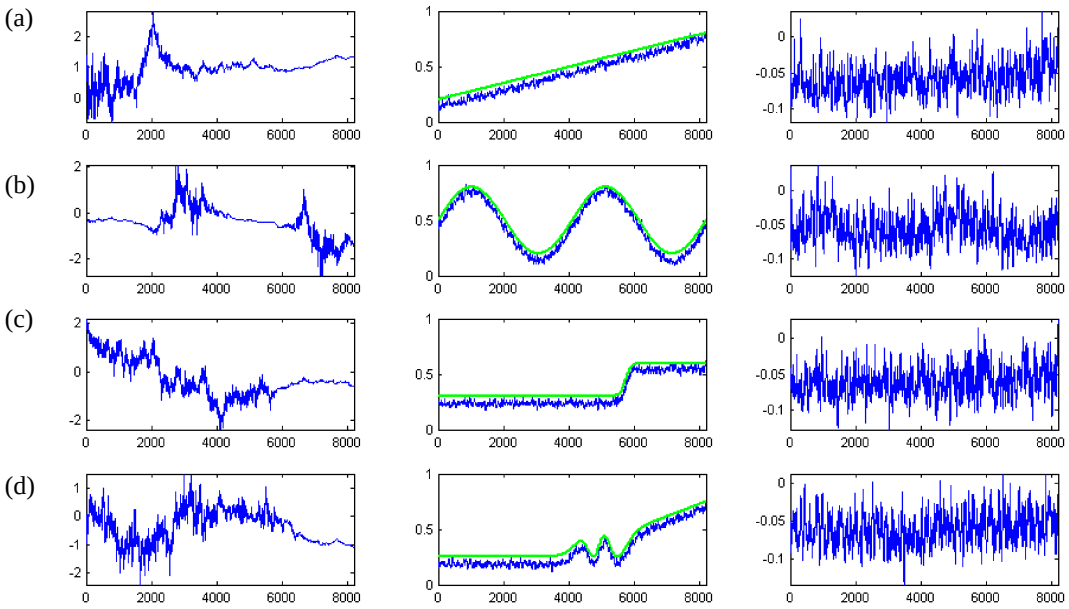

Fig. 2: The application of the GQV algorithm to a simulated path of an mBm with different types of Hurst function H(t): (a) linear (b) periodic (c) logistic (d) synthetic
In the left, the simulated path of the mBm, in the middle, the Hurst function estimated by the GQV algorithm (in blue line) and the theoretical Hurst function (in green line) and in the right, the error function which is the difference between the estimated Hurst function and the theoretical Hurst function.

The results showed that for the different types of the Hurst functions, the estimated Hurst function, represented in blue line, is very close to the theoretical Hurst function, plotted in green line and the error functions' values are almost ranged between -0.1 and 0. We confirm again that the GQV algorithm constitutes an accurate estimator of the Hurst exponent of mBm processes.

APPLICATION TO KTB SONIC LOG DATA

Here, the application of the GQV algorithm is focused on sonic logs data measured at the pilot borehole (`Vorbohrung', VB) drilled for the German Continental Deep Drilling Program (KTB).

This borehole is located in the south-eastern Germany and reaches depths of about 4000m in crystalline basement rocks. The main lithological units characterizing the KTB site are: paragneisses, metabasites and alternations of gneiss and amphibolite, The logs considered in this study are the P-wave velocity (Vp) sonic log and the S-wave velocity (Vs) sonic log data recorded in the depth interval (28.194 - 3990.137 m) with a sampling interval of 0.1524 m (6 inches).

Both velocity logs display an increasing trend of the velocity with depth due to the increasing consolidation of the crystalline rocks. This tendency can be observed on the blue lines fitting the velocity logs.

The trend removal is an important step in the processing of random velocity data [24-26]. In the case of the trends are not eliminated from data, large distortions can occur in the processing of correlation and spectral quantities.

The suppression of trends changes also the raw well data, which are generally non-Gaussian and non-stationary, to be approximately Gaussian and stationary. However, by normalization, the obtained series have zero mean and unit variance. These intermediate operations are likely to yield more accurate Hurst estimations. In the other hand, we have to precise that the GQV algorithm is very efficient in the case of a normalized (or standard) mBm.

In our work, linear trends are fitted using least squares procedures and are removed from the velocity logs. Then, for each log, we examine the corresponding stochastic component s(z) which is given by [26, 27]:

$$s(z) = \frac{V(z) - (V_0 + V_1\ z)}{V_0 + V_1\ z}$$

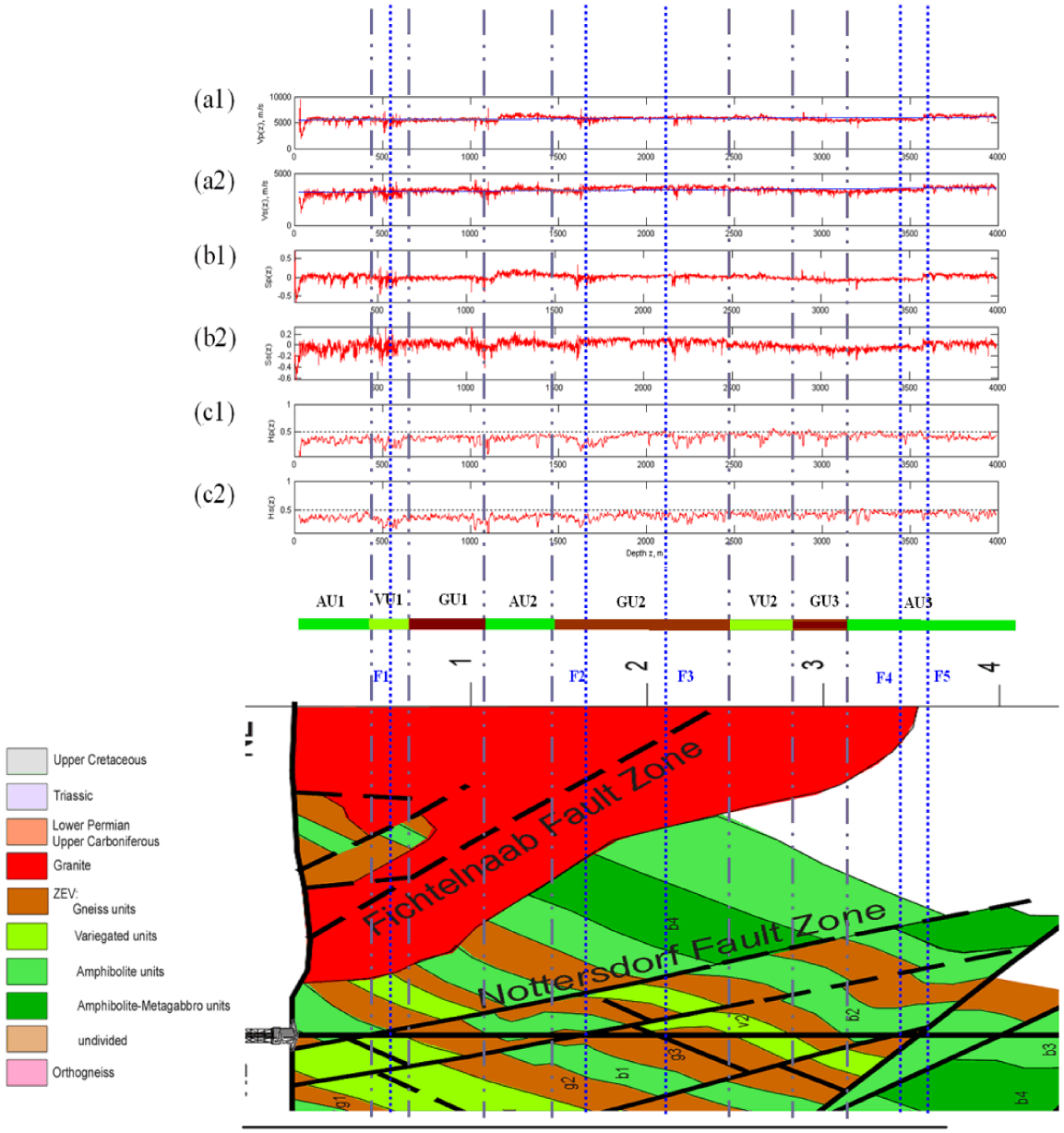

Fig. 3: Results obtained by the application of the GQV algorithm to sonic measurements at the pilot (VB) borehole (a1) & P-wave velocity (Vp(z)) - (a2) S-wave velocity (Vs(z)) (b1) Vp(z)'s stochastic component (Sp(z)) - (b2) Vs(z)'s stochastic component (Ss(z)) (c1) Vp(z)'s Hurst function (Hp(z)) - (c2) Vs(z)'s Hurst function (Hs(z)) (e) lithologic sketch modified from http://icdp.gfz-potsdam.de/html/ktb Blue line: contacts with faults; grey line: lithological changes

Where z is the depth, V_0 and V_1 are coefficients determined by linear regression (least-squares fitting procedures) which are presented in Table 2.

In Figure 2, we present the velocity logs, Vp(z) and Vs(z), shown in red line, with their respective corresponding linear trends, shown in blue line (Figs. 3.a1 & 3.a2), their corresponding stochastic components Sp and Ss (Figs. 3.b1 & 3.b2) and finally their estimated Hurst functions Hp(z) and Hs(z) (Figs. 3.c1 & 3.c2).

Table 2: Least-squares fitting coefficients (V_0 and V_1) related to sonic logs (VB, pilot borehole)

Type	V_0 (m/s)	V_1 (1/s)
VB-Vp	5527	0.1222
VB-Vs	3182	0.1073

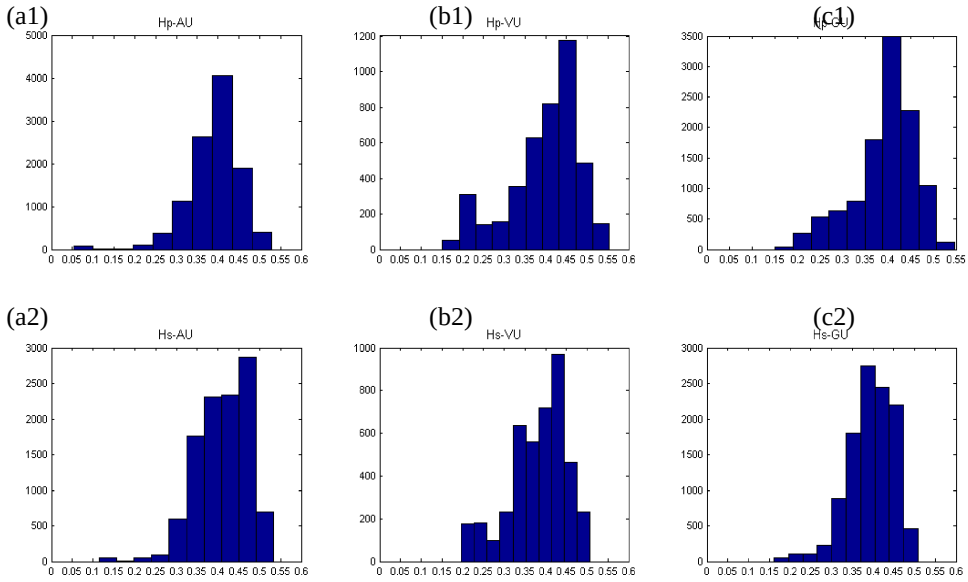

Fig. 4: Histograms of the Hurst values obtained by the GQV algorithm from P and S-wave sonic logs (a1) Hp(z)-AU (b1) Hp(z)-VU (c1) Hp(z)-GU (a2) Hs(z)-AU (b2) Hs(z)-VU (c2) Hs(z)-GU

We observe that the estimated regularity profiles of both sonic logs exhibit a similar form. In addition, the estimated Hurst values are mostly less than 0.5, which leads us to conclude that the investigated sonic logs show anti-persistence property. The velocity variations are then unpredictable.

In order to establish a lithological segmentation on the estimated regularity profiles, we used a geological section crossing the KTB borehole (Fig. 3.e1). The analysis of the Hurst value variation allowed us to identify the following lithological units, whose bounds are shown in grey line, are: AU1-AU2-AU3 (for Amphibolite Units), VU1-VU2 (for Variegated Units) and GU1-GU2-GU3 (for Gneiss Units). Moreover, we confirm the presence of the five faults: F1, F2, F3, F4 & F5, presented in blue line. Indeed, the transition between two adjacent lithological units and the faults' presence are marked by abrupt jumps of the Hurst value.

We observe that in contrast to the Gneiss and Variegated units, the amphibolites units are well recognized on the regularity profiles. This may be due to the fact that the P and S-waves velocities in amphibolites are higher than in the other units. On the other hand, the gneiss and variegated units present close velocities, so it is difficult to distinguish one from other. Concerning the faults, we precise that the faults F2 and F3 are not clearly recognized because they are positioned inside the gneiss unit GU2.

For both estimated Hurst functions related to the velocity logs, we established histograms for each identified unit (Fig. 4). We remark that the histograms corresponding to all the lithological units (AU, VU and GU) for both sonic logs fellow a normal distribution. Moreover, we observe that the means of the Hurst values obtained from Vs Velocity log are larger than those resulted from Vp velocity log, in the case of AU (mean=0.3896 for Hp, mean=0.4117 for Hs) and GU (mean=0.3925 for Hp, mean=0.3958 for Hs). This statement is reversed for the VU unit (mean=0.3970 for Hp, mean=0.3821 for Hs). In overall, the Hurst values mean for the geological units obtained from both velocity logs are close. It is then difficult to characterize a lithological unit by a specific mean Hurst value, but the GQV algorithm still an appropriate tool to delimit the layers basing on the variation of the Hurst function.

However, we pointed out that all the standard-deviation values corresponding to Vp log are slightly larger than those associated to Vs log for each geological unit, but they are generally comparable and small.

CONCLUSION

This study showed that borehole wire-line logs can be assumed as multifractional Brownian motion (mBm) processes which offer the possibility to investigate the local multifractality behavior by the means of the depth-dependent Hurst exponent.

On synthetic logs simulated by Successive Random Additions (SRA) method, we showed that the Generalized Quadratic Variations (GQV) algorithm allowed to accurate Hurst function (or regularity profile) estimations, which are very close to their corresponding theoretical Hurst functions.

Moreover, we demonstrated the potential of the GQV algorithm on P and S-wave velocity sonic logs data recorded at the KTB pilot borehole. The variation of the local Hurst value estimated by this algorithm allowed to position faults and to recognize the geological layers crossed by the borehole.

We conclude that the GQV algorihm may constitute a suitable tool for a lithological segmentation, thus to characterize sub-surface heterogeneities using the estimated regularity profile.

REFERENCES

1. Bean, C.J., 1996. On the cause of 1/f-power spectral scaling in borehole sonic logs. Geophysical Research Letters, 23(22): 3119-3122.
2. Dolan, S.S. and C.J. Bean, 1997. Some remarks on the estimation of fractal scaling parameters from borehole wire-line logs. Geophysical Res. Lett., 24(10): 1271-1274.
3. Dolan, S.S., C.J. Bean and B. Riolet, 1998. The broad-band fractal nature heterogeneity in the upper crust from petrophysical logs. Geophys. J. Int., 132: 489-507.
4. Pilkington, M. and J.P. Todoeschuck, 1991. Naturally smooth inversions with a priori information from well logs, Geophysics, 56(11): 1811-1818.
5. Todoeschuck, J.P., O.G. Jensen and S. Labonte, 1990. Gaussian scaling noise model of seismic reflection sequences: Evidence from well logs, Geophysics, 55: 480-484.
6. Arizabalo, R.D., K. Oleschko, G. Korvin, G. Ronquillo and E. Cedillo-Pardo, 2004. Fractal and cumulative trace analysis of wire-line logs from a well in a naturally fractured limestone reservoir in the Gulf of Mexico. Geofís. Int., 43(3): 467- 476.
7. Arizabalo, R.D., K. Oleschko, G. Korvin, M. Lozada, R. Castrejón and G. Ronquillo, 2006. Lacunarity of geophysical well logs in the Cantarell oil field, Gulf of Mexico, Geofís. Int., 45(2): 99-113.
8. Chamoli, A., A.R. Bansal and V.P. Dimri, 2007. Wavelet and rescaled range approach for the Hurst coefficient for short and long time series, Computers & Geosciences, 33: 83-93.
9. Leonardi, S. and H.J. Kümpel, 1998. Variability of geophysical log data and the signature of crustal heterogeneities at the KTB. Geophys. J. Int., 135: 964-974.
10. Leonardi, S. and H.J. Kümpel, 1999. Fractal variability in super deep borehole implications for the signature of crustal heterogeneities. Tectonophysics, 301: 173-181.
11. Malamud, B.D. and D.L. Turcotte, 1999. Self-affine time series: measures of weak and strong persistence, J. Statistical Planning and Inference, 80: 173-196.
12. Mandelbrot, B.B. and J.W. Van Ness, 1968. Fractional Brownian Motions, Fractional Noises and Applications, SIAM Review, 10: 422-437.
13. Ayache, A. and J. Lévy Véhel, 2000. The Generalized Multifractional Brownian Motion, Statistical Inference for Stochastic Processes, 3: 7-18.
14. Lévy Véhel, J., 1995. Fractal Approaches in Signal Processing, Fractals, 3: 755-775.
15. Peltier, R.F. and J. Lévy Véhel, 1995. Multifractional brownian motion: definition and preliminary results. Rapport De Recherche de l'INRIA, 2645.
16. Ayache, A., S. Cohen and J. Lévy Véhel, 2000. The covariance structure of multifractional Brownian Motion, with Application to Long Range Dependence. ICASSP.
17. Ayache, A. and M.S. Taqqu, 2005. Multifractional Process with Random Exponent. Publ. Mat., 49: 459-486.
18. Ayache, A., S. Jaffard and M.S. Taqqu, 2007. Wavelet construction of generalized multifractional processes. Rev. Mat. Iberoamericana., 23(1): 327-370.
19. Benassi, A., S. Jaffard and D. Roux, 1997. Gaussian processes and pseudodifferential elliptic operators. Rev. Mat. Iberoamericana, 13(1): 19-81.
20. Falconer, K.J., 2002. Tangent fields and the local structure of random fields. J. Theoret. Probab., 15: 731-750.
21. Falconer, K.J., 2003. The local structure of random processes. J. London Math. Soc., 67(2): 657-672.
22. Ayache, A. and J. Lévy-Véhel, 2004. Identification of the pointwise holder exponent of generalized multifractional brownian motion. Stochastic Processes and their Applications, 111: 119-156.
23. Turcotte, D.L., 1997. Fractals and Chaos in Geology and Geophysics. Cambridge University Press, Cambridge, pp: 398.

24. Bendat, J.S. and A.G. Piersol, 1986, Random data, analysis and measurement procedures, 2nd Edition (Revised and Expanded): John Wiley & Sons.
25. Li, X.P., 1998. Wavelet power spectrum analysis of heterogeneities from sonic velocity logs, Geophys. Prospect., 46: 455-475.
26. Shiomi, K., H. Sato and M. Ohtake, 1997. Broad-band power-law spectra of well-log data in Japan. Geophys. J. Int., 130: 57-64.
27. Zaourar, N., L. Briqueu, S. Gaci, M. Hamoudi and D. Gibert, 2006. Sonic Log Analysis with the Continuous Wavelet Transform. Bulletin du Service géologique National. Alger, 17: 161-181.
00. Li, C.F., 2003. Rescaled-range and power spectrum analyses on well logging data. Geophys. J. Int., 153: 201-212.